Journal of Alloys and Compounds 495 (2010) 234–237

Contents lists available at ScienceDirect

Journal of Alloys and Compounds

journal homepage: www.elsevier.com/locate/jallcom

Band gap engineering in PbS nanostructured thin films from near-infrared down to visible range by in situ Cd-doping

S. Thangavel [a], S. Ganesan [b], S. Chandramohan [c,*], P. Sudhagar [d], Yong Soo Kang [d], Chang-Hee Hong [c]

[a] Department of Physics, Muthayammal College of Arts and Science, Namakkal 637 408, India
[b] Department of Physics, Government College of Technology, Coimbatore 641 013, India
[c] School of Semiconductor and Chemical Engineering, Chonbuk National University, Chonju 561-756, South Korea
[d] Energy Materials Laboratory, Department of Chemical Engineering, Hanyang University, Seoul 133-791, South Korea

ARTICLE INFO

Article history:
Received 2 December 2009
Received in revised form 14 January 2010
Accepted 21 January 2010
Available online 4 February 2010

Keywords:
PbS thin films
Cd-doping
Optical band gap
Quantum confinement

ABSTRACT

In this paper, we report on the modification of optical band gap of PbS nanostructured films over a wide spectral range (~475–1000 nm) due to in situ Cd-doping and size confinement. The films investigated in this study are grown by chemical bath deposition (CBD) at different temperatures and the doping was conducted for a fixed impurity concentration. The PbS films grown under optimal deposition conditions are found to crystallize in face centered cubic (fcc) structure with an average crystallite size in the range of 22–27 nm. The estimated optical band gap was in the range of 1.22–1.42 eV, for films grown at different temperatures. Doping was found to influence the film growth and results in a reduction of crystallite size (down to 9 nm). Consequently, quantum size effect becomes pronounced in the Cd-doped PbS films, which lead to a significant enhancement in the optical band gap (up to 2.61 eV). X-ray photoelectron spectroscopy analysis confirms the substitutional doping of Cd into PbS lattice. Band gap modification due to quantum confinement and formation of ternary PbCdS are addressed.

1. Introduction

Lead sulfide (PbS) is a prominent direct narrow gap semiconductor with a room temperature band gap of 0.41 eV and finds a wide range of potential applications in various devices such as infrared photodetectors, optical switches, sensors, and solar cells [1–3]. Because of relatively large Bohr exciton radius of 18 nm [3], its band gap can be engineered over a wide range by reducing the particle size. These properties make the quantum confinement effects more notable in PbS compared to other lead chalcogenides, even for relatively larger particle sizes. In this viewpoint, PbS has been grown in various forms by different techniques such as chemical bath deposition (CBD), vacuum evaporation, spray pyrolysis, electrodeposition, etc. [3–6]. Among these techniques, CBD offers simple, cost effective, and industrially scalable route for the production of high-quality films, without the need for high-deposition temperatures.

Recently, growth of mixed thin film structures based on PbS and CdS ($Pb_{1-x}Cd_xS$ and $Cd_{1-x}Pb_xS$) finds immense interest, because it offers the advantage of tuning the optical and the opto-electronic properties of PbS, viz. band gap, electrical conductivity, thermoelectric power, etc., in a controlled manner [7–9]. In the present work, attempt has been made to prepare PbS and Cd-doped PbS nanostructured films by CBD. Addition of Cd into the bath is found to strongly affect the film growth, which as a consequence controls the optical properties of PbS films. We observed quantum size effect in both pure and Cd-doped PbS films and the results are discussed in detail.

2. Experimental details

Undoped and Cd-doped PbS thin films were deposited on to micro-glass substrates by CBD technique. Bath containing lead acetate ($Pb(CH_3COO)_2{\cdot}3H_2O$) and thiourea ($CH_4N_2S$), in appropriate concentrations, was used for the deposition of PbS films. The pH of the solution was adjusted by adding a small amount of NH_3 (2.21 ml) and Triethanolamine (TEA) was used as a complexing agent. Following this, chemically cleaned micro-glass slides were immersed in the solution for the deposition of PbS films. In this process, deposition of PbS film occurs because of a chemical reaction of controlled sulfur and lead ions in the alkaline solution. First, dissociation of metal complex initiates a slow release of Pb^{2+} ions:

$$[Pb(NH_3)_4]^{2+} \rightarrow 4NH_3 + Pb^{2+} \quad (1)$$

Simultaneously, slow release of sulfur from thiourea takes place via decomposition, according to the following chemical reactions and when it reacts with the Pb^{2+} form a uniform deposit on to the substrate:

$$SC(NH_2)_2 + OH^- \rightarrow SH^- + CH_2N_2 + H_2O \quad (2)$$

$$SH^- + OH^- \rightarrow S^{2-} + H_2O \quad (3)$$

$$Pb^{2+} + S^{2-} \rightarrow PbS \quad (4)$$

Similarly, the deposition of Cd-doped PbS films was achieved by adding an appropriate amount of aqueous solution of cadmium acetate with the reaction

* Corresponding author. Tel.: +82 10 28979827.
E-mail address: scmphysics@gmail.com (S. Chandramohan).

0925-8388/$ – see front matter © 2010 Elsevier B.V. All rights reserved.
doi:10.1016/j.jallcom.2010.01.135

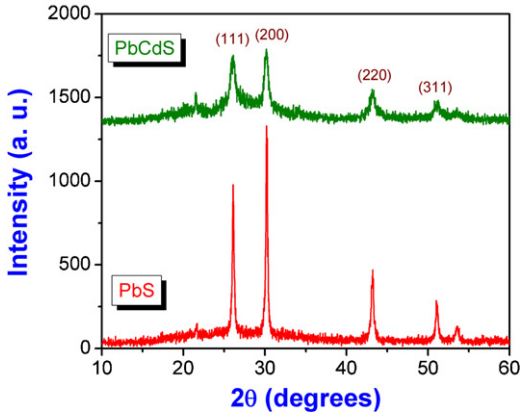

Fig. 1. X-ray diffraction spectra of PbS and PbCdS nanocrystalline thin films deposited at a bath temperature of 85 °C.

mixture and the overall chemical reaction is as follows:

$$1-x[Pb(NH_3)_4]^{2+} + x[Cd(NH_3)_4]^{2+} + SC(NH_2)_2 \xrightarrow{NH_4OH} Pb_{1-x}Cd_xS + 6NH_3 + CO_3{}^{2-} + H_2O \quad (5)$$

Herein, addition of TEA helps to control the release of Pb^{2+} and Cd^{2+}, resulting into the deposition of ternary PbCdS for desired composition. The films deposited in this method were found to be homogeneous and well adhered to the substrate.

The structure of the films was analyzed by XRD with Cu-Kα radiation (λ = 1.5405 Å). X-ray photoelectron spectroscopy (XPS) study was carried out using a VG Microtech (VG Multilab ESCA 2000 system) X-ray photoelectron spectrometer. The experiment was carried out in a high-vacuum chamber under a base pressure of 3×10^{-9} Torr and the samples were excited with Al Kα X-ray radiation of 1487 eV energy. All the spectra reported in this work are referenced to C 1s peak (284.6 eV). The surface morphology of the films was probed by using a JEOL (JSM-6701F) field-emission scanning electron microscopy (FE-SEM). The optical absorbance spectra were recorded by using a UV–vis–NIR spectrophotometer (Lambda 35 model).

3. Results and discussion

Fig. 1 shows the XRD spectra of pure and Cd-doped PbS films deposited at a bath temperature of 85 °C. In the case of PbS films, we observe sharp peaks at $2\theta \approx 26.1°$, 30.2°, 43.2°, and 51.1°. The observed peak positions are consistent with the fcc structure of PbS (JCPDS-ICDD PDF# 5-05920) and they are represented by their corresponding Miller indices in the spectra. The appearance of sharp peaks reveals polycrystalline nature of the films. However, we noticed a small shift (~0.5%) in the position of all the peaks towards higher 2θ values, compared to the standard values of bulk PbS. Such a marginal shift in the diffraction peaks can be attributed to lattice strain resulting due to any structural disorder generated during the film growth [10]. Moreover, the absence of any other peaks corresponding to metallic clusters and/or impurities reveals good quality of the films. Similar results were observed for films deposited at other temperatures. The average crystallite size (D) was estimated using the Debye–Scherrer formula [5]. The value of D was found to be in the range of 22–27 nm (Table 1), for PbS films deposited at different temperatures.

Table 1
Calculated average crystallite size and optical band gap of PbS and PbCdS films deposited at different temperatures.

Temperature (°C)	Crystallite size (nm)		Band gap (eV)	
	PbS	PbCdS	PbS	PbCdS
75	22	12	1.42	2.33
80	25	10	1.37	2.50
85	27	9	1.22	2.61

A comparison of XRD line shapes of PbS and PbCdS films clearly indicates a significant broadening after doping. There are two main possible causes for the peak broadening. The first is increase in heterogeneity of the films due to the occupation of Cd into the host lattice. A second cause is a decrease in crystallite size. It can be mentioned that the stable crystal structure of PbS (fcc) differs from that of CdS (hexagonal close packed). As a result, when Cd^{2+} occupies more and more sites of Pb^{2+} in the host lattice, internal strain would arise, and the crystal structure of the PbCdS solid solution becomes unstable. In order to stabilize the crystal structure, the grain size is reduced to release the strain. As the Cd concentration is increased, the diffraction peaks become broader due to a reduction in the grain size [11]. Similar results are reported for Mn-doped CdS films [11,12]. The value of D calculated for PbCdS films was found to be in the range of 9–11 nm. It is also noted that the intensity of the diffraction peaks decreases after doping (Fig. 1). This can be attributed to doping induced structural disorder in the films [13]. Moreover, we observed a decrease in the lattice d spacing of PbCdS films compared to the corresponding values in PbS films. This confirms the formation of PbCdS; because when Cd^{2+} occupies the Pb^{2+} sites in the lattice, the lattice would undergo a contraction due to smaller ionic radii of Cd^{2+} [14]. This result is in line with the literature where similar results are reported for other ternary systems [11,13].

To further validate the formation of ternary alloy, we performed XPS measurements on a representative undoped and Cd-doped PbS films. Fig. 2 shows the survey scan spectra of the films wherein the presence of core levels corresponding to Pb, S, and Cd confirms the formation of PbS and PbCdS. It should be mentioned that both C 1s and O 1s photoelectron lines are likely resulting from the adsorbed gaseous molecules since nanocrystalline materials exhibit a high surface-to-volume ratio. For a comprehensive understanding of the modifications in the electronic structure of PbS, the high-resolution spectra of principal core levels were analyzed by using a XPS Peak Fitting Program. The detailed procedure of fitting the peaks can be found in an earlier paper [15]. Experimental high-resolution spectra of Pb $4f_{7/2}$, Cd $3d_{5/2}$ and S $2p$ core levels along with their resolved components are shown in Fig. 3. The peaks located at 137.4 and 138.6 eV in the Pb $4f_{7/2}$ core level spectrum of undoped PbS film can be assigned to Pb–S and Pb–O bonding, respectively. These binding energy (BE) values are consistent with the data reported in the literature [16]. The above observation indicates that Pb is in two different chemical environments. However, the BE positions of Pb $4f_{7/2}$ (137.4 eV) and S $2p_{3/2}$ (161.5 eV) confirms the formation of PbS. We observed a downward shift (of approximately 1.1 eV) in

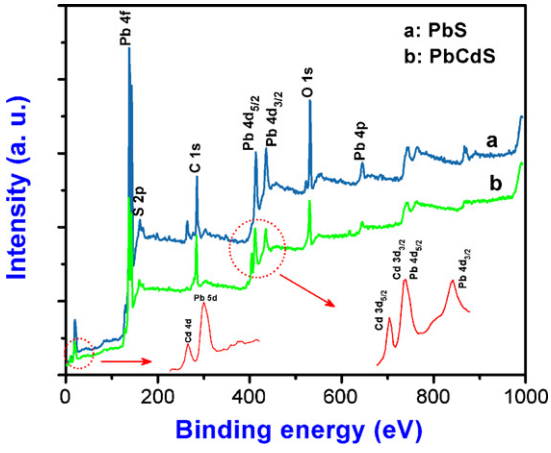

Fig. 2. XPS survey scan spectra of undoped and Cd-doped PbS films. The emergence of additional photoelectron lines corresponding to Cd core levels in the spectrum associated with Cd-doped PbS film is shown explicitly in the insets.

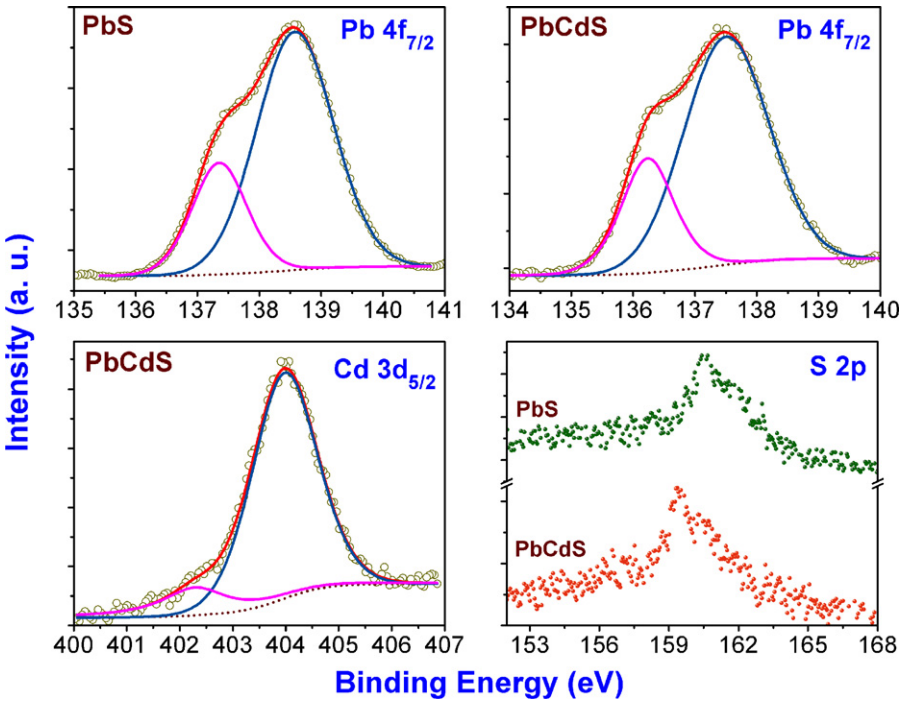

Fig. 3. High-resolution X-ray photoemission spectra of Pb $4f_{7/2}$, Cd $3d_{5/2}$, and S 2s core levels from undoped and Cd-doped PbS films.

the BE position of Pb $4f_{7/2}$ core levels in Cd-doped PbS film. This shift in the BE position and the occurrence of peak at 404 eV in the Cd $3d_{5/2}$ core level spectrum both confirms the formation of PbCdS. In fact, the mobility of Cd^{2+} is higher that that of Pb^{2+}; as a result, Cd have a propensity to occupy the substitutional sites in the PbS lattice and circumvents the formation of any metallic clusters. This result is consistent with the XRD observations discussed earlier. Another low intensity peak at 402.3 eV in the Cd $3d_{5/2}$ core level spectrum is attributed to Cd–O bonding. It is also noted that the Cd $3d_{5/2}$ and the S $2p$ core levels have also shifted towards lower BE after doping.

Fig. 4 shows the SEM images of PbS and PbCdS films grown at 70 °C. It can be seen that the surface of undoped PbS film is composed of pyramidal- and disc-shaped nanocrystals of different dimensions and sizes. It should be noted that the average crystallite sizes deduced from the Scherrer formula are much lower than the grain sizes observable in the SEM pictures. However, grains in the sizes less than a 100 nm are also evident in the micrograph (Fig. 4a). The observed discrepancy can be probably due to the non-spherical geometry of the nanocrystallites. In fact, it is anticipated in the case of nanocrystalline thin films that the domains have a tendency to increase its size near the film surface, thus SEM images representing the surface features of the film, give maximum possible size of grains [17]. On the other hand, crystallite sizes calculated using the XRD data is thickness averaged magnitude, which usually dominated by the smallest crystallites [18]. Similar discrepancy has been reported for various thin films. The addition of Cd into the solution modifies the thin film growth as shown in Fig. 4b. Here, any pyramidal- or disc-shaped structures have not been observed and the morphology of the film shows aggregates of finite particles. Although individual particles are not clearly visible with this magnification, the morphology clearly reveals a strong agglomeration of finite particles.

Fig. 5 exemplifies the absorption spectra of PbS and PbCdS films deposited at a bath temperature of 80 °C. It can be seen from the spectra that Cd-doping results in a strong blue shift in the absorption onset. We observed similar effect for films deposited at other temperatures as well (not shown here). The band gap energy, E_g, was calculated using the Tauc's relation [14], $(\alpha h\upsilon)^{1/n} = A(h\upsilon - E_g)$, where A is a constant and n is equal to 1/2 for direct allowed transitions. The estimation of band gap from the plot of $(\alpha h\upsilon)^2$ verses

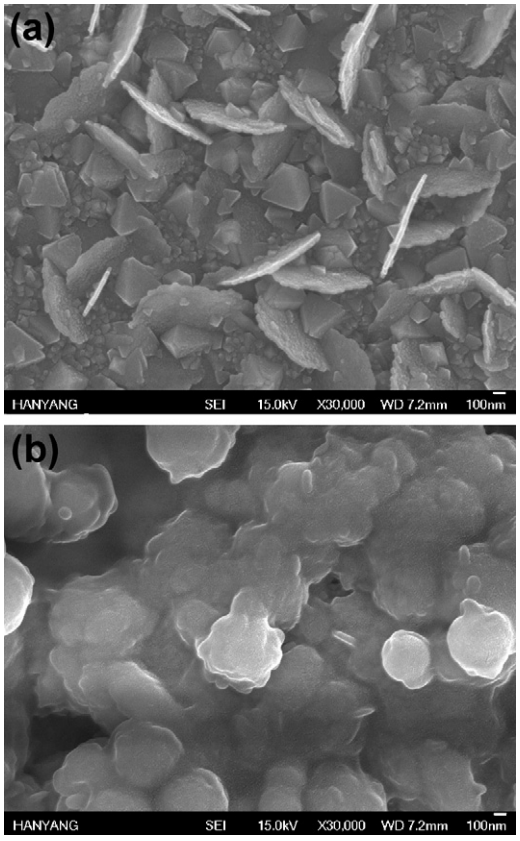

Fig. 4. Plan-view SEM images of (a) PbS and (b) PbCdS films deposited at 70 °C.

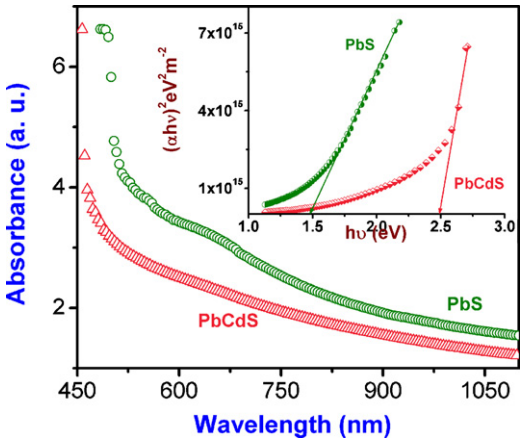

Fig. 5. Absorption spectra of PbS and PbCdS films deposited at 80 °C. Inset shows the estimation of band gap from Tauc's plot.

$h\upsilon$ is shown in the inset of Fig. 5. Band gap values are obtained by extrapolating the linear part of the absorption curves to intercept the energy axis ($\alpha h\upsilon = 0$). The estimated E_g of PbS films is found to be 1.42, 1.37, and 1.22 eV, respectively, for films grown at 75, 80, and 85 °C. The E_g of PbS films, having a small crystallite size in the range of 22–27 nm (Table 1), is found much larger than that of bulk PbS (0.41 eV), which could be due to quantum size effects [5,11]. Similar results are reported for CBD grown PbS films [4]. Moreover, the decrease in E_g with increase in temperature can be attributed to grain size effect [10,19], because we observe an increase in the crystallite size with increasing bath temperature.

The band gap of PbCdS films was also estimated and the values are given in Table 1. In this case, the estimated E_g values are found to be 2.33, 2.50, and 2.61 eV, respectively, for films deposited at 75, 80, and 85 °C. This clearly indicates a considerable increase in the band gap as a result of Cd-doping. Doping of PbS with Cd is expected to alter the optical band gap between 0.41 (E_g of PbS) and 2.43 eV (E_g of CdS) in the resulting ternary PbCdS alloy. Thus, the observed large modification in the band gap confirms the formation of ternary PbCdS alloy and the existence of strong quantum confinement in this system. This could probably be attributed to a decrease in the effective mass and an increase in the binding energy over that in PbS nanocrystals, similar to the results observed in the case of $Pb_{1-x}Fe_xS$ nanoparticle films by Joshi et al. [20]. As mentioned earlier, we observe a systematic decrease in the crystallite size with increasing bath temperature. Since the estimated mean crystallite size in this case being approximately half the value of the exciton Bohr radius in PbS, we observe a strong confinement in PbCdS films. Besides, the crystallite size decreases with increasing bath temperature, which is contrary to the result observed for PbS films. This leads us to understand that when bath temperature increases more Pb^{2+} ions are replaced by Cd^{2+}, which as a result increases the internal strain. As already mentioned, this built in strain would result in a reduction of grain size. In this situation, the composition x of the $(PbS)_{1-x}(CdS)_x$ solid solution would also increase, and hence an increase in the band gap is anticipated. In fact, Sood et al. [21] have derived a simple relation to define the band gap of $Pb_{1-x}Cd_xS$, based on their experimental results. According to Ref. [21], the fundamental absorption edge is written as $E_g(Pb_{1-x}Cd_xS) = E_g(PbS) + 1.80x$. Though this cannot be directly applied to our present case, it obviously enlightens that the large shift in the band gap of PbCdS in our case is a combined result of confinement effect and formation of ternary PbCdS.

4. Conclusions

In situ Cd-doping is found to induce considerable modifications in the optical band gap of PbS nanocrystalline thin films. It is experimentally shown that the band gap of PbS can be engineered over a wide range (1.22–2.61 eV) by changing the deposition conditions and introducing the Cd metal impurities. We observed strong quantum confinement effect in the case of PbCdS films. These properties could potentially be utilized to harvest maximum photon energy from the sunlight to enhance the photovoltaic performance. Since the band gap could be tuned to cover the entire visible region, PbCdS nanostructured films would be a promising candidate for solar cell applications.

Acknowledgments

Two of the authors (PS and YS Kang) acknowledge Korea Science and Engineering Foundation for financial support granted through Nano R&D program (2007-02866) and Engineering Research Center program (R11-2008-088-01001-0).

References

[1] S.A. McDonald, G. Konstantatos, S. Zhang, P.W. Cyr, E.J.D. Klem, L. Levina, E.H. Sargent, Nature Mater. 4 (2005) 138.
[2] K.W. Johnston, A.G. Pattantyus-Abraham, J.P. Clifford, S.H. Myrskog, D.D. MacNeil, L. Levina, E.H. Sargent, Appl. Phys. Lett. 92 (2008) 151115.
[3] Shu Fen Wang, Feng Gu, Meng Kai Lu, Langmuir 22 (2006) 398.
[4] R.K. Joshi, A. Kanjilal, H.K. Sehgal, Appl. Surf. Sci. 221 (2004) 43.
[5] K.K. Nanda, S.N. Sahu, Adv. Mater. 13 (2001) 280.
[6] G. Zhou, M. Lü, Z. Xiu, S. Wang, H. Zhang, Y. Zhou, S. Wang, J. Phys. Chem. B 110 (2006) 6543.
[7] E. Rabinovich, E. Wachtel, G. Hodes, Thin Solid Films 517 (2008) 737.
[8] A. Ounissi, N. Ouddai, S. Achour, Eur. Phys. J. Appl. Phys. 37 (2007) 241.
[9] E. Pentia, V. Draghici, G. Sarau, B. Mereu, L. Pintilie, F. Sava, M. Popescu, J. Electrochem. Soc. 151 (2004) G729.
[10] P. Prathap, N. Revathi, Y.P. Venkata Subbaiah, K.T. Ramakrishna Reddy, J. Phys. Condens. Matter 20 (2008) 035205.
[11] C.T. Tsai, S.H. Chen, D.S. Chuu, Phys. Rev. B 54 (1996) 11555.
[12] D.H. Kim, D.J. Lee, N.M. Kim, S.J. Lee, T.W. Kang, Y.D. Woo, D.J. Fu, J. Appl. Phys. 101 (2007) 094111.
[13] H.K. Yadav, K. Sreenivas, R.S. Katiyar, V. Gupta, J. Phys. D: Appl. Phys. 40 (2007) 6005.
[14] N. Badera, B. Godbole, S.B. Srivastava, P.N. Vishwakarma, L.S.S. Chandra, D. Jain, M. Gangrade, T. Shripathi, V.G. Sathe, V. Ganesan, Appl. Surf. Sci. 254 (2008) 7042.
[15] S. Chandramohan, R. Sathyamoorthy, P. Sudhagar, D. Kanjilal, D. Kabiraj, K. Asokan, V. Ganesan, T. Shripathi, U.P. Deshpande, Appl. Phys. A 94 (2009) 703.
[16] S. Chen, W. Liu, Mater. Chem. Phys. 98 (2006) 183.
[17] G. Korotcenkov, A. Cornet, E. Rossinyol, J. Arbiol, V. Brinzari, Y. Blinov, Thin Solid Films 471 (2005) 310.
[18] K.P. Acharya, J.R. Skuza, R.A. Lukaszew, C. Liyanage, B. Ullrich, J. Phys.: Condens. Matter 19 (2007) 196221.
[19] A.U. Ubale, A.R. Junghare, N.A. Wadibhasme, A.S. Daryapurkar, R.B. Mankar, V.S. Sangawar, Turk. J. Phys. 31 (2007) 279.
[20] R.K. Joshi, A. Kanjilal, H.K. Sehgal, Nanotechnology 14 (2003) 809.
[21] A.K. Sood, J.N. Zemel, J. Appl. Phys. 49 (1978) 5292.